Recursive parametric tests for multichannel adaptive signal detection

K.J. Sohn, H. Li and B. Himed

Abstract: The problem of detecting a multichannel signal in spatially and temporally coloured disturbances is considered. The parametric Rao and parametric generalised likelihood ratio test detectors, recently developed by modelling the disturbance as a multichannel autoregressive (AR) process, have been shown to perform well with limited or even no range training data. These parametric detectors, however, assume that the model order of the multichannel AR process is known a priori to the detector. In practice, the model order has to be estimated by some model order selection technique. Meanwhile, a standard non-recursive implementation of the parametric detectors is computationally intensive since the unknown parameters have to be estimated for all possible model orders before the best one is identified. To address these issues, herein the joint model order selection, parameter estimation and target detection are considered. We present recursive versions of the aforementioned parametric detectors by integrating the multichannel Levinson algorithm, which is employed for recursive and computationally efficient parameter estimation, with a generalised Akaike Information Criterion for model order selection. Numerical results show that the proposed recursive parametric detectors, assuming no knowledge of the model order, yield a detection performance nearly identical to that of their non-recursive counterparts at significantly reduced complexity.

1 Introduction

Space–time adaptive processing (STAP) has proven to be an effective approach for signal detection in the presence of strong interference/clutter, for example an airborne radar environment [1, 2]. Conventional STAP detectors, such as the Reed, Mallett and Brennan (RMB) detector [3], Kelly's generalised likelihood ratio test (GLRT) [4], the adaptive matched filter (AMF) detector [5–7], and the adaptive coherence estimator (ACE) detector [8–10], involve estimating and inverting a space–time covariance matrix obtained from target-free training data. This may impose excessive training and computational burdens especially when the joint space–time dimension is large. It is therefore of great interest to reduce the training and computational requirements of such STAP detectors for practical and real-time applications.

Parametric model-based STAP detectors have received significant interest in recent years [11–18]. Specifically, the parametric adaptive matched filter (PAMF), which was developed by modelling the disturbance as a multichannel autoregressive (AR) process, was shown to outperform the aforementioned covariance matrix-based STAP detectors, providing improved detection performance with reduced training data requirements [11, 12]. More recently, the PAMF detector has been shown to be closely related to a parametric Rao detector [15, 16]. Specifically, both

detectors share an identical test statistic form, although the PAMF uses only training signals for parameter estimation, whereas the parametric Rao detector uses both training and test signals for that purpose [15, 16]. One advantage of the parametric Rao detector is that it can handle the training-free case, in which case it derives parameter estimates exclusively from the test signal. Moreover, a parametric GLRT, which also models the disturbance as a multichannel AR process, has been developed in [17, 18]. The parametric GLRT has been found to yield improved detection performance over the parametric Rao detector with a somewhat higher complexity. Both the parametric Rao and parametric GLRT detectors have been shown to asymptotically achieve constant false alarm rate. In addition, the asymptotic distribution of their test statistics has been obtained in closed-form, which can be used to set the test threshold and determine the detection and false alarm probabilities. Furthermore, unlike the covariance matrix-based STAP detectors, both the parametric Rao and parametric GLRT detectors are found to perform well with limited or even no range training data [17, 18]. As such, these detectors are particularly useful for airborne radar target detection in heterogeneous or dense-target environments, where range training is usually limited.

The PAMF, parametric Rao and parametric GLRT detectors, however, were developed by assuming that the model order of the multichannel AR process is known to the detector a priori. In practice, the model order has to be estimated using some model order selection technique, such as the generalised Akaike Information Criterion (GAIC), minimum description length, or others [19]. Since most of these model order selection techniques require estimates of the unknown parameters for each possible model order before the best one is identified, a standard non-recursive implementation of the parametric detectors turns out to be computationally intensive.

In this paper, we consider a joint model order selection, parameter estimation and target detection procedure for STAP applications. We note that the parameter estimates of a multichannel AR process for all model orders can be efficiently obtained by recursively solving a set of multichannel Yule–Walker equations using the multichannel Levinson algorithm [20, 21]. The multichannel Levinson algorithm yields parameter estimates for a particular model order at every recursion. Information criteria such as the GAIC can then be conveniently computed. As such, the estimation of the model order is naturally integrated. We follow the above approach and develop recursive versions of the parametric Rao and parametric GLRT detectors. The recursive parametric detectors utilise the Yule–Walker parameter estimates obtained by using the multichannel Levinson algorithm with the biased autocorrelation function (ACF) estimate [20, 21]. Our development of the recursive versions of the parametric detectors integrated with the GAIC for model order selection is well motivated since the multichannel Levinson algorithm is computationally efficient and the model order is not required to be known to the detectors. Numerical results show that the Yule–Walker parameter estimates are asymptotically equivalent to the maximum likelihood (ML) estimates originally used in the non-recursive parametric Rao [15, 16] and parametric GLRT [17, 18] detectors. It is also observed that the recursive parametric detectors perform nearly identically to the corresponding non-recursive parametric detectors, even though the former assumes no knowledge of the model order, whereas the latter assumes the exact model order.

The rest of the paper is organised as follows. Section 2 contains the data model and problem statement. The non-recursive parametric Rao and parametric GLRT detectors with known model order are summarised in Section 3. Section 4 contains our recursive parametric Rao and parametric GLRT detectors with unknown model order. Numerical results are presented in Section 5, followed by our conclusions in Section 6.

Notation: Vectors (matrices) are denoted by boldface lower (upper) case letters, all vectors are column vectors, superscripts $(\cdot)^{\mathrm{T}}$ and $(\cdot)^{\mathrm{H}}$ denote transpose and complex conjugate transpose, respectively, $\boldsymbol{I}$ denotes the identity matrix, $\mathcal{CN}(\boldsymbol{\mu}, \boldsymbol{R})$ denotes the multivariate complex Gaussian distribution with mean $\boldsymbol{\mu}$ and covariance matrix $\boldsymbol{R}$, $\mathbb{C}$ denotes the complex number field and finally $(\cdot)^{\dagger}$ denotes the Moore-Penrose pseudo-inverse.

2 Data model and problem statement

Consider the problem of detecting a known multichannel signal with unknown amplitude in the presence of spatially and temporally coloured disturbance (e.g. [1]).

$$
\begin{aligned}
H_0: \quad & \boldsymbol{x}_0 = \boldsymbol{d}_0 \\
H_1: \quad & \boldsymbol{x}_0 = \alpha \boldsymbol{s} + \boldsymbol{d}_0
\end{aligned}
\tag{1}
$$

where all vectors have $JN \times 1$ dimensions with J denoting the number of spatial channels and N the number of temporal observations. The test signal $\boldsymbol{x}_0$ contains a disturbance signal $\boldsymbol{d}_0$ and possibly a target signal $\alpha \boldsymbol{s}$, where $\boldsymbol{s}$ denotes the target steering vector which is assumed known and α the unknown complex amplitude. In addition to the test signal $\boldsymbol{x}_0$, there may be a set of target-free training or secondary signals $\boldsymbol{x}_k = \boldsymbol{d}_k \in \mathbb{C}^{JN \times 1}$, $k = 1, \ldots, K$,

that can be exploited to assist in the target detection process. In this paper, we consider both cases with or without range training data; in the latter case, we set $K = 0$. The disturbance signals $\{\boldsymbol{d}_k\}_{k=0}^{K}$ are assumed to be independent and identically distributed with distribution $\mathcal{CN}(0, \boldsymbol{R})$, where $\boldsymbol{R} \in \mathbb{C}^{JN \times JN}$ is the unknown space–time covariance matrix.

Let us decompose the $JN \times 1$ space–time vector $\boldsymbol{x}_k$ into a series of $J \times 1$ spatial vectors $\boldsymbol{x}_k(n)$ as follows

$$
\boldsymbol{x}_k = [\boldsymbol{x}_k^{\mathrm{T}}(0), \ldots, \boldsymbol{x}_k^{\mathrm{T}}(N-1)]^{\mathrm{T}}
\tag{2}
$$

Let $\boldsymbol{d}_k$ and $\boldsymbol{s}$ be similarly decomposed into $\boldsymbol{d}_k(n) \in \mathbb{C}^{J \times 1}$ and $\boldsymbol{s}(n) \in \mathbb{C}^{J \times 1}$, respectively. Then, we can rewrite the hypothesis testing using the above spatial vectors indexed by n (time):

$$
\begin{aligned}
H_0: \quad & \boldsymbol{x}_0(n) = \boldsymbol{d}_0(n), \quad n = 0, \ldots, N-1 \\
H_1: \quad & \boldsymbol{x}_0(n) = \alpha \boldsymbol{s}(n) + \boldsymbol{d}_0(n), \quad n = 0, \ldots, N-1
\end{aligned}
\tag{3}
$$

Furthermore, we follow a parametric approach as in [11, 12, 15–18], which models the disturbance signal $\boldsymbol{d}_k(n)$, as a J-channel AR (P) process with unknown model order P.

$$
\boldsymbol{d}_k(n) = -\sum_{i=1}^{P} \boldsymbol{A}^{\mathrm{H}}(i) \boldsymbol{d}_k(n-i) + \boldsymbol{\varepsilon}_k(n), \quad k = 0, 1, \ldots, K
\tag{4}
$$

where $\{\boldsymbol{A}^{\mathrm{H}}(i)\}_{i=1}^{P}$ denote the unknown $J \times J$ AR coefficient matrices and $\boldsymbol{\varepsilon}_k(n)$ the $J \times 1$ spatial noise vectors that are temporally white but spatially coloured: $\boldsymbol{\varepsilon}_k(n) \sim \mathcal{CN}(0, \boldsymbol{Q})$, where $\boldsymbol{Q} \in \mathbb{C}^{J \times J}$ denotes the unknown spatial covariance matrix.

The problem of interest is to develop parametric detectors for the above composite hypothesis testing problem (1) or (3), using the test signal $\boldsymbol{x}_0$ and training signals $\{\boldsymbol{x}_k\}_{k=1}^{K}$ (if any). We reiterate that the model order P is assumed unknown to the detector in this paper, whereas the original developments of the PAMF, parametric Rao and parametric GLRT detectors all assume that P is known [11, 12, 15–18]. A distinctive feature of this work is that we consider computationally efficient solutions to this joint order selection problem, parameter estimation and target detection problem.

3 Non-recursive parametric Rao and parametric GLRT detectors with known model order

For easy reference and to facilitate our development of the recursive parametric detectors, we provide a brief summary of the parametric Rao and GLRT detectors in this section. These detectors are two different solutions to the problem stated in Section 2 when the model order P is known [15–18]. The parametric Rao detector is computationally simpler, but the parametric GLRT offers improved performance. Both detectors first find the ML estimates of the unknown parameters, which are next used to compute the test statistics. The likelihood functions under the null and alternative hypotheses are parameterised by the signal amplitude α, the AR coefficients $\boldsymbol{A}^{\mathrm{H}} = [\boldsymbol{A}^{\mathrm{H}}(1), \ldots, \boldsymbol{A}^{\mathrm{H}}(P)] \in \mathbb{C}^{J \times JP}$, and spatial covariance matrix $\boldsymbol{Q}$. Note that under the null hypothesis we have $\alpha = 0$. Given $\boldsymbol{A}$, the steering vector and test signal can be temporally whitened through the following

inverse (i.e. moving average) filtering.

$$\tilde{s}(n) = s(n) + \sum_{i=1}^{P} A^{H}(i)s(n-i) \qquad (5)$$

$$\tilde{x}_0(n) = x_0(n) + \sum_{i=1}^{P} A^{H}(i)x_0(n-i) \qquad (6)$$

This is an important observation exploited by the parametric Rao and parametric GLRT detectors that are summarised as follows.

The parametric GLRT is given by [17, 18]

$$T_{\mathrm{GLRT}} = 2L \ln \frac{|\hat{\boldsymbol{Q}}_{\mathrm{ML,\,0}}|}{|\hat{\boldsymbol{Q}}_{\mathrm{ML,\,1}}|} \underset{H_0}{\overset{H_1}{\gtrless}} \gamma_{\mathrm{GLRT}} \qquad (7)$$

where $L = (K+1)(N-P)$ and γ_{GLRT} denotes the corresponding test threshold. The ML estimates of the spatial covariance matrix under the null and alternative hypotheses, $\hat{\boldsymbol{Q}}_{\mathrm{ML,0}}$ and $\hat{\boldsymbol{Q}}_{\mathrm{ML,1}}$ are given by

$$\hat{\boldsymbol{Q}}_{\mathrm{ML,0}} = \hat{\boldsymbol{Q}}(\alpha)|_{\alpha=0} \qquad (8)$$

$$\hat{\boldsymbol{Q}}_{\mathrm{ML,1}} = \hat{\boldsymbol{Q}}(\alpha)|_{\alpha=\hat{\alpha}_{\mathrm{ML}}} \qquad (9)$$

The α-dependent $\hat{\boldsymbol{Q}}(\alpha)$ is given by

$$\hat{\boldsymbol{Q}}(\alpha) = \frac{1}{L}(\hat{\boldsymbol{R}}_{xx}(\alpha) - \hat{\boldsymbol{R}}_{yx}^{H}(\alpha)\hat{\boldsymbol{R}}_{yy}^{-1}(\alpha)\hat{\boldsymbol{R}}_{yx}(\alpha)), \qquad (10)$$

where the α-dependent correlation matrices are

$$\hat{\boldsymbol{R}}_{xx}(\alpha) = \sum_{k=1}^{K} \sum_{n=P}^{N-1} x_k(n)x_k^{H}(n)$$
$$+ \sum_{n=P}^{N-1} [x_0(n) - \alpha s(n)][x_0(n) - \alpha s(n)]^{H} \qquad (11)$$

$$\hat{\boldsymbol{R}}_{yy}(\alpha) = \sum_{k=1}^{K} \sum_{n=P}^{N-1} y_k(n)y_k^{H}(n)$$
$$+ \sum_{n=P}^{N-1} [y_0(n) - \alpha t(n)][y_0(n) - \alpha t(n)]^{H} \qquad (12)$$

$$\hat{\boldsymbol{R}}_{yx}(\alpha) = \sum_{k=1}^{K} \sum_{n=P}^{N-1} y_k(n)x_k^{H}(n)$$
$$+ \sum_{n=P}^{N-1} [y_0(n) - \alpha t(n)][x_0(n) - \alpha s(n)]^{H} \qquad (13)$$

with $t(n)$ and $y_k(n)$ denoting the regression subvectors formed from the steering vector $s(n)$ and test signal $x_k(n)$, respectively: $t(n) = [s^{T}(n-1), \ldots, s^{T}(n-P)]^{T} \in \mathbb{C}^{JP \times 1}$ and $y_k(n) = [x_k^{T}(n-1), \ldots, x_k^{T}(n-P)]^{T} \in \mathbb{C}^{JP \times 1}$, $k = 0, \ldots, K$. The ML estimate of α under the alternative hypothesis, which is used in (9), is given by

$$\hat{\alpha}_{\mathrm{ML}} = \arg\min_{\alpha} |\hat{\boldsymbol{R}}_{xx}(\alpha) - \hat{\boldsymbol{R}}_{yx}^{H}(\alpha)\hat{\boldsymbol{R}}_{yy}^{-1}(\alpha)\hat{\boldsymbol{R}}_{yx}(\alpha)| \qquad (14)$$

The parametric Rao test is given by [15, 16]

$$T_{\mathrm{Rao}} = \frac{2\left|\sum_{n=P}^{N-1} \hat{\tilde{s}}^{H}(n)\hat{\boldsymbol{Q}}_{\mathrm{ML,0}}^{-1}\hat{\tilde{x}}_0^{H}(n)\right|^2}{\sum_{n=P}^{N-1} \hat{\tilde{s}}^{H}(n)\hat{\boldsymbol{Q}}_{\mathrm{ML,0}}^{-1}\hat{\tilde{s}}_0^{H}(n)} \underset{H_0}{\overset{H_1}{\gtrless}} \gamma_{\mathrm{Rao}} \qquad (15)$$

where γ_{Rao} denotes the test threshold. The temporally whitened steering vector $\hat{\tilde{s}}^{H}(n)$ and test signal $\hat{\tilde{x}}_0^{H}(n)$ are

obtained by replacing A^{H} with its ML estimate under H_0

$$\hat{A}_{\mathrm{ML,0}}^{H} = -\hat{\boldsymbol{R}}_{yx}^{H}(\alpha)\hat{\boldsymbol{R}}_{yy}^{-1}(\alpha)|_{\alpha=0} \qquad (16)$$

in (5) and (6), respectively.

The Rao test is shown to be asymptotically equivalent to the GLRT but may be inferior to the latter when the data size is small. In addition, the Rao test is obtained based upon a low-order Taylor expansion of the GLRT, an approximation which is only valid for weak signals [22]. As such, the performance of the parametric Rao detector degrades when the weak signal assumption is violated. The parametric GLRT was developed as an improved detector to deal with the above issues. However, the cost function of the ML amplitude estimator in (14) is highly nonlinear. Newton-like iterative nonlinear searches are generally used to find the ML amplitude estimate. Another suboptimum but computationally more efficient estimator, referred to as the asymptotic ML (AML) estimator, was developed in [17, 18]. The AML estimator, which was found to yield similar performance to the ML estimator, can be implemented as follows:

Step 1: First, compute a least-squares (LS) amplitude estimate $\hat{\alpha}_{\mathrm{LS}} = s^{H}x_0/s^{H}s$. Then, determine an estimate $\hat{A}_{\mathrm{LS}}^{H}$ of A^{H} as follows.

$$\hat{A}_{\mathrm{LS}}^{H} = \hat{\boldsymbol{R}}_{yx}^{H}(\hat{\alpha}_{\mathrm{LS}})\hat{\boldsymbol{R}}_{yy}^{-1}(\hat{\alpha}_{\mathrm{LS}}) \qquad (17)$$

which can be shown to be statistically consistent [17, 18].
Step 2: Compute the temporally whitened signals $\hat{\tilde{x}}_k(n)$ and $\hat{\tilde{s}}(n)$ by replacing A^{H} with the LS AR coefficient estimate $\hat{A}_{\mathrm{LS}}^{H}$ in (5) and (6), respectively. Then, obtain the AML amplitude estimate $\hat{\alpha}_{\mathrm{AML}}$ by using

$$\hat{\alpha}_{\mathrm{AML}} = \frac{\mathrm{tr}(\hat{\tilde{\boldsymbol{S}}}^{H}\boldsymbol{\Psi}^{-1}\hat{\tilde{\boldsymbol{X}}}_0)}{\mathrm{tr}(\hat{\tilde{\boldsymbol{S}}}^{H}\boldsymbol{\Psi}^{-1}\hat{\tilde{\boldsymbol{S}}})}, \qquad (18)$$

where $\hat{\tilde{\boldsymbol{S}}} = [\hat{\tilde{s}}(P), \ldots, \hat{\tilde{s}}(N-1)] \in \mathbb{C}^{J \times (N-P)}$, $\hat{\tilde{\boldsymbol{X}}}_k = [\hat{\tilde{x}}_k(P), \ldots, \hat{\tilde{x}}_k(N-1)] \in \mathbb{C}^{J \times (N-P)}$ and

$$\boldsymbol{\Psi} = \hat{\tilde{\boldsymbol{X}}}_0 \boldsymbol{P}^{\perp} \hat{\tilde{\boldsymbol{X}}}_0^{H} + \sum_{k=1}^{K} \hat{\tilde{\boldsymbol{X}}}_k \hat{\tilde{\boldsymbol{X}}}_k^{H} \qquad (19)$$

with $\boldsymbol{P}^{\perp}$ denoting the projection matrix projecting to the orthogonal complement of the range of $\hat{\tilde{\boldsymbol{S}}}^{H}: \boldsymbol{P}^{\perp} = \boldsymbol{I} - \boldsymbol{P} = \boldsymbol{I} - \hat{\tilde{\boldsymbol{S}}}^{H}(\hat{\tilde{\boldsymbol{S}}}^{H})^{\dagger} \in \mathbb{C}^{(N-P) \times (N-P)}$.
Step 3: Find the AML estimate of the spatial covariance matrix by substituting $\hat{\alpha}_{\mathrm{AML}}$ for α in (10).

Recall that the parametric Rao and parametric GLRT detectors utilise both the test and training signals for the parameter estimation. As a result, they are functional even without range training data [17, 18]. The capability to handle the training-free detection is a unique and desirable attribute of the parametric detectors which is not shared by other existing detectors including the PAMF detector. Nevertheless, we need a way to efficiently find an accurate estimate of the model order P.

4 Recursive parametric tests with unknown model order

A standard non-recursive implementation of the parametric detectors is computationally intensive since the parameter estimation for the underlying parametric model has to be repeated for all possible model orders before the best one

is identified. Therefore there is a need to develop more efficient solutions for joint model order selection, parameter estimation and detection.

We present herein recursive versions of the parametric Rao and parametric GLRT detectors. The multichannel Levinson algorithm is used to recursively solve a set of multichannel Yule–Walker equations for model order $p = 1, 2, \ldots, P_{\max}$, where $P_{\max}$ is an upper bound on the model order P. Interestingly, the complexity involved in the above procedure, which provides parameter estimates for all $P_{\max}$ model orders, has lower complexity than that involved in solving a single model order $p = P_{\max}$ by the ML approach (see Section 4.5 for details). Given these parameter estimates for all possible p, an information criterion such as the GAIC can be conveniently utilized to identify the best model order as well as the associated estimates of A, Q and α. These parameter estimates are then used to compute the final test statistics for the parametric Rao and GLRT detectors. In the following, we discuss the details of the proposed joint approach.

4.1 Parameter estimation by the multichannel Levinson algorithm

Assume that $x(n)$ is a J-channel AR(P) process as described in (4). Estimates of the unknown parameters can be obtained by solving the multichannel Yule–Walker equations given by [20, 21]

$$
R(m) = \begin{cases} -\sum_{i=1}^{P} A^{H}(i)R(m-i), & m \geq 1 \\ -\sum_{i=1}^{P} A^{H}(i)R(-i) + Q, & m = 0 \end{cases} \tag{20}
$$

where the autocorrelation matrix is defined as

$$
R(m) = E[x(n)x^{H}(n-m)] \tag{21}
$$

In matrix form, the multichannel Yule–Walker equations become

$$
\mathcal{A}_P \mathcal{R} = \begin{bmatrix} Q & 0 & \cdots & 0 \end{bmatrix} \tag{22}
$$

where the block matrix $\mathcal{A}_P$ contains the multichannel AR coefficients and $\mathcal{R}$ is a block Toeplitz matrix.

$$
\mathcal{A}_P = \begin{bmatrix} I & A_P^{H}(1) & \ldots & A_P^{H}(P) \end{bmatrix} \tag{23}
$$

$$
\mathcal{R} = \begin{bmatrix} R(0) & \cdots & R(P) \\ R(-1) & \cdots & R(P-1) \\ \vdots & \ddots & \vdots \\ R(-P) & \cdots & R(0) \end{bmatrix} \tag{24}
$$

The multichannel Levinson algorithm can be used to recursively solve the above multichannel Yule–Walker equations for different model orders as follows [20, 21].

The multichannel Levinson algorithm begins with the following initial conditions.

$$
Q_0^{f} = Q_0^{b} = R(0) \tag{25}
$$

$$
\mathcal{A}_0 = \mathcal{B}_0 = I \tag{26}
$$

$$
K_0^{fH} = K_0^{bH} = I \tag{27}
$$

Henceforth, the superscripts f and b denote the forward and backward directions of a linear prediction process used by the Levinson algorithm, the subscript denotes the order of the linear predictor, $\mathcal{A}$ and $\mathcal{B}$ denote the block row matrices

formed by the forward and backward AR coefficient matrices, respectively, and K denotes the reflection coefficient matrix.

Given the pth order forward and backward AR coefficient matrices $\mathcal{A}_p$ and $\mathcal{B}_p$, the forward and backward reflection coefficient matrices for the $(p+1)$th order linear predictors are computed by

$$
K_{p+1}^{fH}(p+1) = -\Delta_{p+1}(Q_p^{b})^{-1} \tag{28}
$$

$$
K_{p+1}^{bH}(p+1) = -\nabla_{p+1}(Q_p^{f})^{-1}, \tag{29}
$$

where Δ_{p+1} and ∇_{p+1} are defined as

$$
\Delta_{p+1} = \sum_{i=0}^{p} K_p^{fH}(i)R(p+1-i) \tag{30}
$$

$$
\nabla_{p+1} = \sum_{i=0}^{p} K_p^{bH}(i)R(i-p-1) \tag{31}
$$

Next, we update the forward and backward AR coefficient matrices for the $(p+1)$th order predictors as follows.

$$
\mathcal{A}_{p+1} = [\mathcal{A}_p, \quad 0] + K_{p+1}^{fH}(p+1)[0, \quad \mathcal{B}_p] \tag{32}
$$

$$
\mathcal{B}_{p+1} = [0, \quad \mathcal{B}_p] + K_{p+1}^{bH}(p+1)[\mathcal{A}_p, \quad 0] \tag{33}
$$

Finally, we update the forward and backward prediction error covariance matrices for the $(p+1)$-th order predictors.

$$
Q_{p+1}^{f} = Q_p^{f} + K_{p+1}^{fH}(p+1)\nabla_{p+1} \tag{34}
$$

$$
Q_{p+1}^{b} = Q_p^{b} + K_{p+1}^{bH}(p+1)\Delta_{p+1} \tag{35}
$$

which completes the pth recursion of the multichannel Levinson algorithm. Note that the solutions to the pth order multichannel Yule–Walker equations are $\mathcal{A}_p$, and Q_p^{f}.

In practice, the space–time covariance matrix $R(m)$ in the multichannel Yule–Walker equations should be replaced by some estimate. The biased ACF estimate given by

$$
\hat{R}(m) = \frac{1}{N} \sum_{n=0}^{N-1-m} x(n+m)x^{H}(n) \tag{36}
$$

is usually recommended since it guarantees that the matrix $\mathcal{R}$ is non-negative definite [20, 21].

4.2 AR model order selection

Model order selection for parametric models is a classical research topic and has been investigated for various models (e.g. [19, 21] and references therein). Herein, we consider the GAIC, which has been observed to yield good performance results for model order selection (e.g. [23]). The GAIC chooses the model order p that minimises

$$
W(p) = V(p) + \eta(p) \tag{37}
$$

where $V(p)$ is the minimum negative log-likelihood function and $\eta(p)$ is a penalty term that penalises increasing model order [19]. The minimum negative log-likelihood function can be shown to be

$$
V(p) = J(K+1)(N-p)\ln(e\pi) + (K+1)
$$
$$
\times (N-p)\ln|\hat{Q}| \tag{38}
$$

where the dependence on p is made explicit. The penalty

term typically takes the form as [19]

$$\eta(p) = 2cJ^2 p \ln(\ln(K+1)(N-p)) \tag{39}$$

where $c \geq 1$ is a parameter of user choice. It has been found that (37) along with (39) usually provides a consistent model order estimation [19].

4.3 Recursive parametric Rao test

Based on the above recursive parameter estimation and model order selection techniques, the parametric Rao test can be implemented in a recursive manner as follows.

Step 1: Obtain the biased ACF estimate according to (36)

$$\hat{\boldsymbol{R}}(m) = \frac{1}{N(K+1)} \sum_{k=0}^{K} \sum_{n=0}^{N-1-m} \boldsymbol{x}_k(n+m)\boldsymbol{x}_k^{\mathrm{H}}(n) \tag{40}$$

$$m = 0, 1, \ldots, P_{\max}$$

Note that both the training and test signals are used to obtain the ACF estimate.

Step 2: Initialisation: Set $p = 0$ and initialise the forward and backward prediction error covariance matrices, $\boldsymbol{Q}_0^{\mathrm{f}}$ and $\boldsymbol{Q}_0^{\mathrm{b}}$, and the forward and backward AR coefficient matrices, $\mathcal{A}_0$ and $\mathcal{B}_0$, as in (25) and (26). Compute the GAIC $W(0)$ for the 0-th model order by using (37).

Step 3a: Compute the forward and backward reflection coefficient matrices for the $(p+1)$th order linear predictors, $\boldsymbol{K}_{p+1}^{\mathrm{fH}}(p+1)$ and $\boldsymbol{K}_{p+1}^{\mathrm{bH}}(p+1)$, by using (28) and (29).

Step 3b: Update the forward and backward AR coefficient matrices for the $(p+1)$-th order predictors, $\mathcal{A}_{p+1}$ and $\mathcal{B}_{p+1}$, by using (32) and (33). Update the forward and backward prediction error covariance matrices for the $(p+1)$-th order predictors, $\boldsymbol{Q}_{p+1}^{\mathrm{f}}$ and $\boldsymbol{Q}_{p+1}^{\mathrm{b}}$, by using (34) and (35).

Step 3c: Compute the GAIC $W(p+1)$ for the $(p+1)$-th model order, by using (37).

  – If $p = 0$, increase p by 1 and go back to *Step 3a*;
  – else if $W(p+1) \geq W(p)$, go to *Step 4*;
  – otherwise, increase p by 1 and go back to *Step 3a*.

The following upper bound can be imposed for model order selection [12]

$$p \leq \left\lfloor \frac{3\sqrt{N}}{J} \right\rfloor \tag{41}$$

where $\lfloor \cdot \rfloor$ rounds a real-valued number towards zero.

Step 4: The order estimate $\hat{P}$ is p (i.e. the final value of the above recursion index). For the selected model order $\hat{P} = p$, obtain the parameter estimates

$$\hat{A}^{\mathrm{H}}(i) = A_{\hat{P}}^{\mathrm{H}}(i), \quad i = 1, 2, \ldots, \hat{P} \tag{42}$$

$$\hat{\boldsymbol{Q}} = \boldsymbol{Q}_{\hat{P}}^{\mathrm{f}} \tag{43}$$

Compute the parametric Rao test statistic (15) by replacing the ML parameter estimates (16) and (8) with the obtained Yule–Walker solutions (42) and (43), respectively. Finally, the test statistic is compared with a test threshold to decide if the target is present. The test threshold can be determined by using the asymptotic analysis in [15, 16].

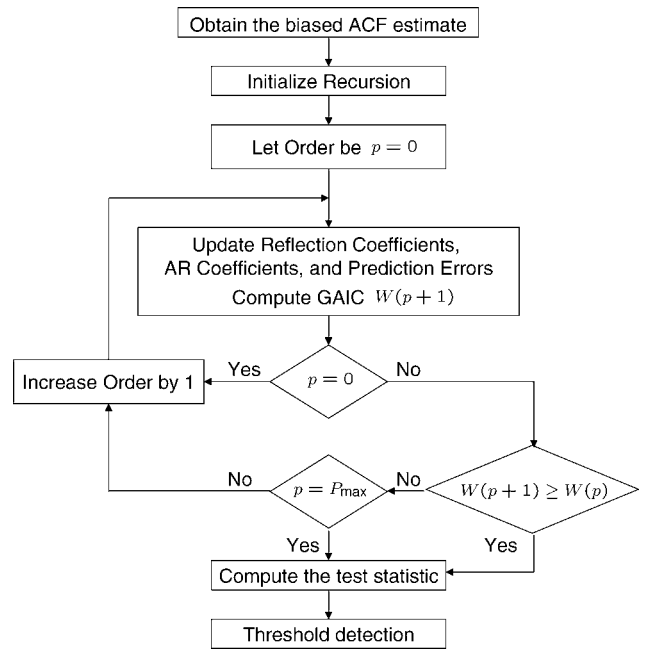The recursive parametric Rao test is summarised in Fig. 1.

Fig. 1 *Summary of recursive parametric Rao test*

4.4 Recursive parametric GLRT

Recursive implementation of the parametric GLRT is more involved than the recursive parametric Rao test. The reason is that finding the ML estimate of α, which is required by the parametric GLRT, is nonlinear even with a known model order [17, 18, 24]. To circumvent the problem, we consider a recursive parametric GLRT by using the model order estimate obtained by the recursive parametric Rao test.

The recursive implementation of the parametric GLRT can be summarised as follows.

Step 1: Find the spatial covariance matrix estimate $\hat{\boldsymbol{Q}}_0$ under H_0 and the model order estimate $\hat{P}$ by using the multi-channel Levinson algorithm in the same manner as in the recursive parametric Rao test.

Step 2: Using the model order estimate $\hat{P}$ obtained in Step 1, find the amplitude estimate $\hat{\alpha}$ by either (14) or (18). Next, obtain the spatial covariance matrix estimate $\hat{\boldsymbol{Q}}_1$ by using $\hat{\alpha}$ and $\hat{P}$. Specifically, the spatial covariance matrix estimate $\hat{\boldsymbol{Q}}_1$ can be obtained by running the multichannel Levinson algorithm a second time (with $\hat{P}$ recursions) along with the following modified ACF estimate.

$$\hat{\boldsymbol{R}}(m) = \frac{1}{N(K+1)} \left\{ \sum_{n=0}^{N-1-m} \check{\boldsymbol{x}}_0(n+m)\check{\boldsymbol{x}}_0^{\mathrm{H}}(n) \right.$$
$$\left. + \sum_{k=1}^{K} \sum_{n=0}^{N-1-m} \boldsymbol{x}_k(n+m)\boldsymbol{x}_k^{\mathrm{H}}(n) \right\} \tag{44}$$

where $\check{\boldsymbol{x}}_0(n) = \boldsymbol{x}_0(n) - \hat{\alpha}\boldsymbol{s}(n)$.

Step 3: Compute the test statistic (7) by replacing the ML parameter estimates (8) and (9) with the Yule–Walker solutions $\hat{\boldsymbol{Q}}_0$ and $\hat{\boldsymbol{Q}}_1$, respectively. Finally, the test statistic is compared with a test threshold to decide if the target is present.

4.5 Complexity

We provide a brief discussion on the complexity involved in the recursive parametric Rao test versus its non-recursive counterpart. Since the recursive and non-recursive implementations differ only in parameter estimation (they share identical steps in signal whitening and calculating the test statistic), we only compare the complexity involved in finding estimates of the AR coefficients A and the spatial covariance matrix Q. Tables 1 and 2 contain a summary of the number of flops involved in the major steps of the recursive and, respectively, non-recursive parameter estimation. For a quick comparison, suppose $(K+1)N > JP_{max}$. Then, it can be seen from Tables 1 and 2 that the recursive parameter estimation, which yields parameter estimates for all model orders, has a overall complexity of $O(J^2 P_{max}(K+1)N)$, whereas the overall complexity of the non-recursive estimation is $O(J^2 P_{max}^3 (K+1)N)$, which is P_{max}^2 times higher.

Similar conclusions can be made for the parametric GLRT since, just like the parametric Rao test, the recursive and non-recursive implementations differ only in how parameter estimates are obtained.

5 Numerical results

In this section, we present simulation results to illustrate the performance of the proposed techniques. The disturbance signal is generated as a multichannel AR(2) process (i.e. $P = 2$) with randomly selected AR coefficients A and a spatial covariance matrix Q. These parameters are set to ensure that the AR process is stable and Q is a valid covariance matrix, but otherwise randomly selected. The steering vector s corresponds to a uniform equi-spaced linear array with $J = 4$ and randomly selected normalised spatial and Doppler frequencies (see [12]). The

Table 1: Complexity of the Yule–Walker estimator with the multichannel Levinson algorithm for model orders $p = 1, \ldots, P_{max}$ (recursive implementation)

Equation	Flops	Remark
(40)	$O(J^2 P_{max}(K+1)N)$	one time calculation
(28), (29)	$O(J^3(p+2))$	at pth recursion
(32), (33)	$O(J^3 p)$	at pth recursion
(34), (35)	$O(J^3)$	at pth recursion
subtotal	$O(J^3 p)$	at pth recursion
total	$O(J^2 P_{max}(K+1)N) + O(J^3 P_{max}^2)$ $\simeq O(J^2 P_{max}(K+1)N)$	for $p = 1, \ldots, P_{max}$

Table 2: Complexity of the ML estimator for model orders $p = 1, \ldots, P_{max}$ (non-recursive implementation)

Equation	Flops	Remark
(11)	$O(J^2(K+1)(N-p))$	for model order p
(12)	$O(J^2 p^2(K+1)(N-p))$	for model order p
(13)	$O(J^2 p(K+1)(N-p))$	for model order p
(10)	$O(J^3(p^3+p^2+p))$	for model order p
subtotal	$O(J^2 p^2(K+1)N) + O(J^3 p^3)$ $\simeq O(J^2 p^2(K+1)N)$	for model order p
total	$O(J^2 P_{max}^3(K+1)N)$	for $p = 1, \ldots, P_{max}$

signal-to-interference-plus-noise ratio (SINR) is defined as

$$\mathrm{SINR} = |\alpha|^2 \boldsymbol{s}^{\mathrm{H}} \boldsymbol{R}^{-1} \boldsymbol{s} \qquad (45)$$

where the $JN \times JN$ space–time covariance matrix can be uniquely determined once A^{H} and Q are selected.

5.1 Estimation

We first examine the estimation performance of the solutions to the multichannel Yule–Walker equations. Since Q is a matrix, we define the following metric.

$$\xi(\boldsymbol{Q}) = \frac{1}{J^2} \mathrm{tr}\left\{ E\left[\left(\hat{\boldsymbol{Q}} - \boldsymbol{Q}\right)^{\mathrm{H}} \left(\hat{\boldsymbol{Q}} - \boldsymbol{Q}\right) \right] \right\} \qquad (46)$$

which is the average of the mean squared errors (MSEs) of all elements of the matrix. For brevity, the above metric is referred as the MSEs henceforth.

Figs. 2 and 3 depict the MSE of the spatial covariance matrix estimate Q against the number of temporal observations N. We consider the Yule–Walker estimate obtained by using the multichannel Levinson algorithm with the corresponding ML estimate (8). Fig. 2 shows the case without
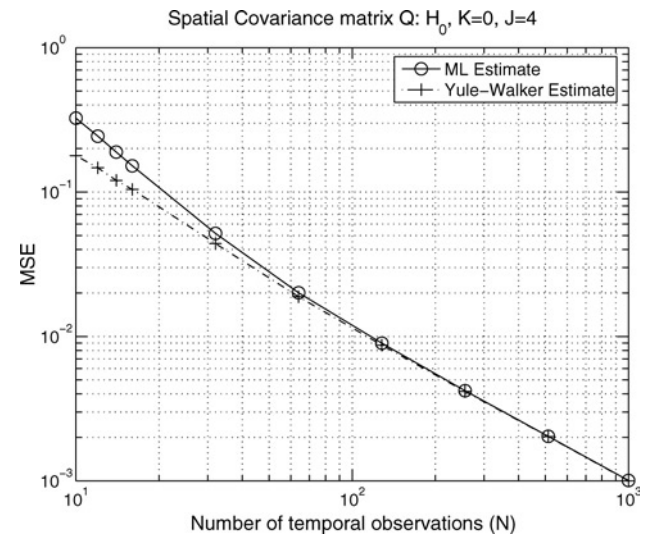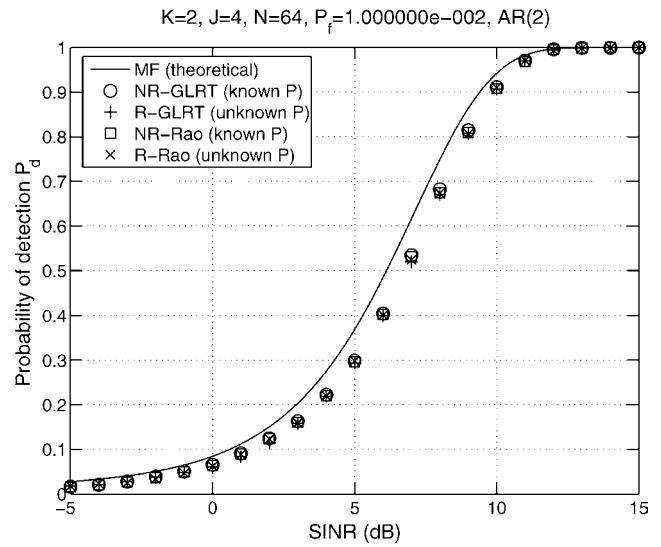
Fig. 2 *MSE of spatial covariance matrix estimate against the number of temporal observations N when K = 0 and J = 4*
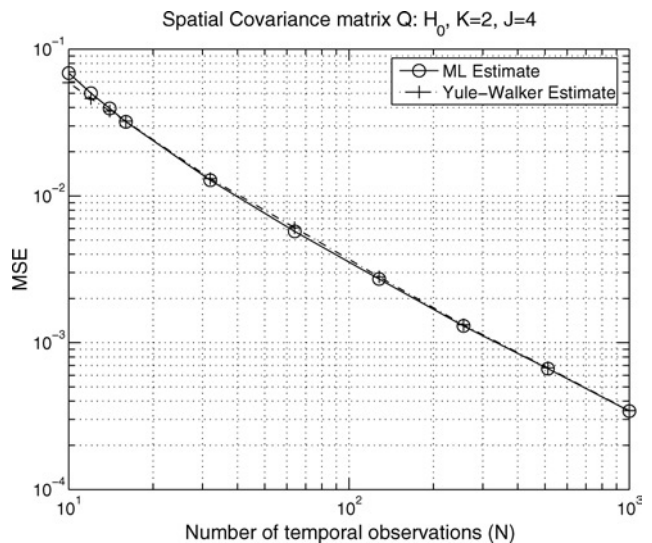
Fig. 3 *MSE of spatial covariance matrix estimate against the number of temporal observations N when K = 2 and J = 4*
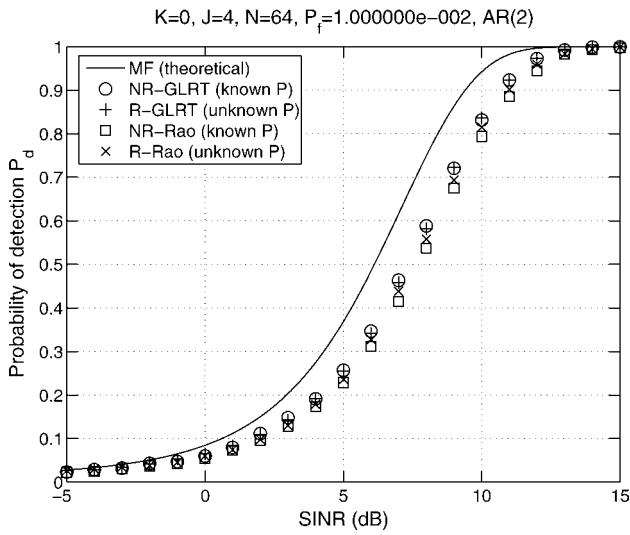
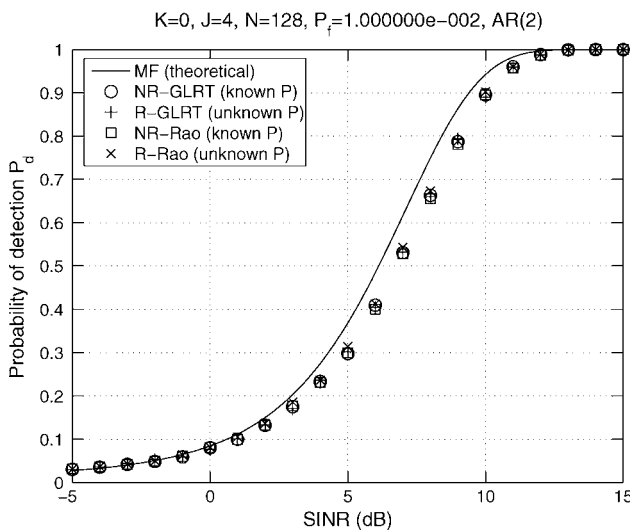**Fig. 4** *Probability of detection P_d against SINR when $K = 0$, $J = 4$, $N = 64$, $P = 2$ and $P_f = 0.01$*

Fig. 6 *Probability of detection P_d against SINR when $K = 2$, $J = 4$, $N = 64$, $P = 2$ and $P_f = 0.01$*

range training data ($K = 0$), whereas Fig. 3 corresponds to the case with limited range training data ($K = 2$). It is observed that the Yule–Walker estimate is asymptotically (for large N and/or large K) equivalent to the ML estimate, although the performance of the Yule–Walker estimate may be different when the data size is small. Fig. 2 shows that the Yule–Walker estimate performs slightly better than the ML estimate, when the number of temporal observations N is small and no range training data are available ($K = 0$). Although it is generally believed that the ML estimate is more accurate than the Yule–Walker estimate (e.g., [25]), with an extremely small data size as considered in this example (e.g. $N = 10$, $K = 0$), either one of the two estimators can slightly outperform the other depending upon the choice of the AR parameters. It should also be noted that the bias of the Yule–Walker estimate (because of the use of the biased ACF estimate) can be significant [25]. Fig. 3 shows that the Yule–Walker estimate performs almost identically to the ML estimate when range training data are used ($K = 2$). It is also observed that the Yule–Walker and ML estimates improve as the range training data (K) and/or temporal observation size (N) increases.
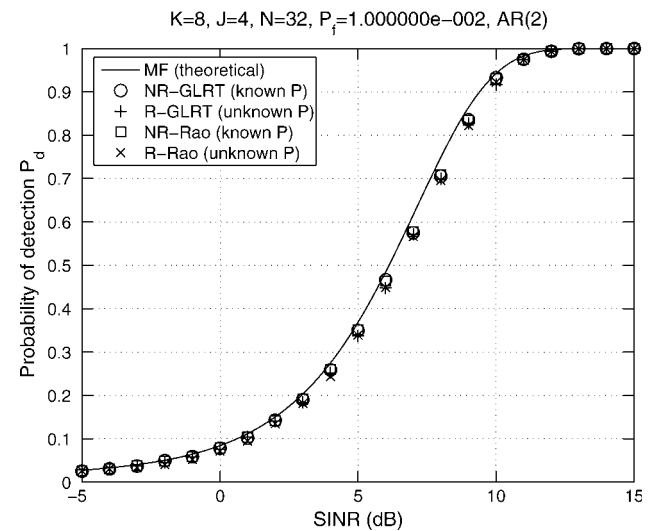
5.2 Detection

We next examine the detection performance of the recursive parametric Rao and GLRT detectors. For the recursive parametric GLRT detector, the AML instead of the ML estimate of α is used since the detection difference between the two is negligible (see [17, 18]), although the AML is computationally simpler. Also included in the comparison is the ideal matched filter (MF), which assumes the exact knowledge of $\boldsymbol{R}$ and is used only as a baseline for comparison. In all examples, we set the probability of false alarm $P_f = 0.01$. Recursive and non-recursive are denoted by 'R' and 'NR', respectively, in the figures. For example, recursive and non-recursive parametric GLRT detectors are denoted by R-GLRT and NR-GLRT, respectively.

Figs. 4–7 depict the probability of detection of various detectors against the SINR for the recursive parametric detector with unknown model order P and their non-recursive counterparts with known P. Figs. 4 and 5 show the case without range training data ($K = 0$), and Figs. 6 and 7 correspond to the case with limited range training data ($K = 2$ and 8). We see that in general, the performance of the recursive parametric detectors with unknown P is

Fig. 5 *Probability of detection P_d against SINR when $K = 0$, $J = 4$, $N = 128$, $P = 2$ and $P_f = 0.01$*

Fig. 7 *Probability of detection P_d against SINR when $K = 8$, $J = 4$, $N = 32$, $P = 2$ and $P_f = 0.01$*

nearly identical to that of their non-recursive counterpart with known P. This is particularly true for the cases shown in Figs. 5–7, where the data size is relatively large (large N with $K = 0$, or a moderate N with non-zero K). On the other hand, it is observed in Fig. 4 that the recursive parametric Rao detector performs slightly better than the non-recursive parametric Rao detector when the temporal observation is small and no range training data is available ($K = 0$ and $N = 64$). This is probably because the Yule–Walker parameter estimate is slightly more accurate than the ML estimate in this case (see Fig. 2).

6 Conclusions

We have presented recursive versions of the parametric Rao and parametric GLRT detectors, utilising the multichannel Levinson algorithm to solve the multichannel Yule–Walker equations recursively and find the estimates of the unknown parameters, along with a GAIC for model order selection. Numerical results show that the Yule–Walker estimate obtained by using the multichannel Levinson algorithm along with the biased ACF estimate is asymptotically equivalent to the ML estimate originally used in the non-recursive parametric Rao and parametric GLRT detectors. It is also shown that the proposed recursive parametric detectors that assume no knowledge about the model order perform almost identically as the corresponding non-recursive parametric detectors with perfect knowledge of the model order, although the formers have reduced computational complexity.

7 Acknowledgment

8 References

1 Ward, J.: 'Space-time adaptive processing for airborne radar', Technical Report 1015, Lincoln Laboratory, MIT, December 1994

2 Klemm, R.: 'Principles of space-time adaptive processing' (The Institute of Electrical Engineers, London, UK, 2002)

3 Reed, I.S., Mallett, J.D., and Brennan, L.E.: 'Rapid convergence rate in adaptive arrays', *IEEE Trans. Aerosp. Electron. Syst.*, 1974, **10**, (6), pp. 853–863

4 Kelly, E.J.: 'An adaptive detection algorithm', *IEEE Trans. Aerosp. Electron. Syst.*, 1986, **22**, pp. 115–127

5 Cai, L., and Wang, H.: 'On adaptive filtering with the CFAR feature and its performance sensitivity to non-Gaussian interference'. Proc.

24th Annul Conf. Information Sciences and Systems, Princeton, NJ, March 1990, pp. 558–563

6 Chen, W., and Reed, I.S.: 'A new CFAR detection test for radar', *Digit. Signal Process.*, 1991, **1**, (4), pp. 198–214

7 Robey, F.C., Fuhrmann, D.R., Kelly, E.J., and Nitzberg, R.: 'A CFAR adaptive matched filter detector', *IEEE Trans. Aerosp. Electron. Syst.*, 1992, **28**, (1), pp. 208–216

8 McWhorter, L.T., and Scharf, L.L.: 'Adaptive matched subspace detectors and adaptive coherence estimators'. Proc. 30th Asilomar Conf. Signals, Systems, and Computers, Pacific Grove, CA, November 1996, pp. 1114–1117

9 Kraut, S., and Scharf, L.L.: 'The CFAR adaptive subspace detector is a scale-invariant GLRT', *IEEE Trans. Signal Process.*, 1999, **47**, (9), pp. 2538–2541

10 Kraut, S., Scharf, L.L., and McWhorter, L.T.: 'Adaptive subspace detectors', *IEEE Trans. Signal Process.*, 2001, **49**, (1), pp. 1–16

11 Rangaswamy, M., and Michels, J.H.: 'A parametric multichannel detection algorithm for correlated non-Gaussian random processes'. Proc. 1997 IEEE National Radar Conf., Syracuse, NY, May 1997, pp. 349–354

12 Román, J.R., Rangaswamy, M., Davis, D.W., Zhang, Q., Himed, B., and Michels, J.H.: 'Parametric adaptive matched filter for airborne radar applications', *IEEE Trans. Aerosp. Electron. Syst.*, 2000, **36**, (2), pp. 677–692

13 Swindlehurst, A.L., and Stoica, P.: 'Maximum likelihood methods in radar array signal processing', *Proc. IEEE*, 1998, **86**, pp. 421–441

14 Li, J., Liu, G., Jiang, N., and Stoica, P.: 'Moving target feature extraction for airborne high-range resolution phased-array radar', *IEEE Trans. Signal Process.*, 2001, **49**, (2), pp. 277–289

15 Li, H., Sohn, K.J., and Himed, B.: 'The PAMF detector is a parametric Rao test'. Proc. 39th Asilomar Conf. Signals, Systems, and Computers, Pacific Grove, CA, November 2005

16 Sohn, K.J., Li, H., and Himed, B.: 'Parametric Rao test for multichannel adaptive signal detection', *IEEE Trans. Aerosp. Electron. Syst.*, 2007, **43**, (3), (accepted for publication)

17 Sohn, K.J., Li, H., and Himed, B.: 'Parametric GLRT for multichannel adaptive signal detection'. Proc. 4th IEEE Workshop on Sensor Array and Multi-channel Processing (SAM06), Waltham, MA, 12–14 July 2006

18 Sohn, K.J., Li, H., and Himed, B.: 'Parametric GLRT for multichannel adaptive signal detection', *IEEE Trans. Signal Process*, 2007, **55**, (11), pp. 5351–5360

19 Söderström, T., and Stoica, P.: 'System identification' (Prentice Hall International, London, UK, 1989)

20 Marple, S.L.: 'Digital spectral analysis with applications' (Prentice Hall, Englewood Cliffs, NJ, 1987)

21 Kay, S.M.: 'Modern spectral estimation: theory and application' (Prentice Hall, Englewood Cliffs, NJ, 1988)

22 Kay, S.M.: 'Fundamentals of statistical signal processing: detection theory' (Prentice Hall, Upper Saddle River, NJ, 1998)

23 Li, J., and Stoica, P.: 'Efficient mixed-spectrum estimation with applications to target feature extraction', *IEEE Trans. Signal Process.*, 1996, **44**, (2), pp. 281–295

24 Sohn, K.J., Li, H., and Himed, B.: 'Amplitude estimation of multichannel signal in spatially and temporally correlated noise'. Proc. Progress in Electromagnetics Research Symp. 2006 (PIERS 2006), Cambridge, MA, March 2006

25 Stoica, P., and Moses, R.L.: 'Introduction to spectral analysis' (Prentice Hall, Upper Saddle River, NJ, 1997)